

Observations of delayed-choice quantum eraser using a continuous wave laser

Byoung S. Ham

Center for Photon Information Processing, Gwangju Institute of Science and Technology

123 Chumdangwagi-ro, Buk-gu, Gwangju 61005, S. Korea

(Submitted on May 28, 2022; bham@gist.ac.kr)

Abstract

Quantum superposition is the heart of quantum mechanics, satisfying complementarity theory between the particle and wave natures of a physical entity such as a photon or atom. Delayed choice of which-path information of a photon in an interferometer has been intensively studied for violation of the cause-effect relation, resulting in a mysterious quantum feature. Here, experimental demonstrations of the delayed-choice quantum eraser are presented using coherent photons of a continuous wave laser to understand the quantum features, where the interferometer comprises a set of polarizing beam splitters to lock indistinguishable photon characteristics. For the delayed-choice quantum eraser, the output photons are measured via polarization projection onto a rotated polarizer, resulting in the retrieval of quantum superposition of a photon in the orthogonally polarized interferometer.

Introduction

Quantum superposition between two random bases of a physical entity such as a single photon and an atom in an interferometric system is the heart of quantum mechanics as mentioned by Dirac [1] and Feynman [2]. The role of measurements for quantum entities is in the controlled choices of the random bases, resulting in the mysterious quantum features of delayed choice [3] and a quantum eraser [4-8], violating the cause-effect relation in classical physics. Delayed-choice phenomena regard which-path information of the physical entity in an interferometric system. Knowing which-path information results in a pure classical system composed of individual and independent particles, prohibiting quantum superposition. Delayed choice of the which-path information, however, can convert the distinguishable (classical) system into an indistinguishable (quantum) system, resulting in retrieval of interference fringes. This phenomenon is the original concept of the quantum eraser as proposed by Scully and Drühl in 1982 [4,5]. Here, a coherence approach is conducted for the delayed-choice quantum eraser with coherent photons in a completely locked noninterfering Mach-Zehnder interferometer (MZI) composed of two polarizing beam splitters (PBSs). For theoretical analysis, the wave nature of a photon is used to understand the observed quantum features, where both relative phase and polarization bases of the superposed photon are critical. Because an interferometric system does not distinguish whether the input light is quantum (entangled or sub-Poisson distributed) or classical (coherent or thermal) for the interference fringes, the continuous wave (cw) laser scheme is rooted in the single photon self-interference [9].

Over the last few decades, delayed-choice and quantum-eraser experiments have been intensively conducted using classical particles of thermal light [10] and quantum particles of antibunched [11,12] or entangled photons [7,8,13]. The delayed-choice and quantum eraser experiments have mainly focused on the particle nature of quantum mechanics using quantum particles, where the phase information of individual photons has not been carefully considered by definition. In the typical single photon-based delayed-choice experiments for a quantum eraser, the photon's distinguishability is preset in an interferometric system, resulting in no interference fringes of output measurements [7,11]. In this case, retrieval of interference in either individual intensity [11] or coincidence detection [7,14] for the output measurements is evidence of the quantum feature in a space-like separation manner. Neglecting the coincidence scheme of entanglement generation, the present scheme shown in Fig. 1 is equivalent to those of Refs. 7 and 14. Even though Ref. 7 has no PBS, it has the same mechanism as the PBS-based one [14] for the same quantum superposition of polarization bases. However, unlike Refs. 7 and 14, Fig. 1 uses coherent photons of a cw laser without coincidence detections. Because the original purpose of the delayed-choice experiments is for the first-order intensity correlation, the coincidence detection is optional for different purposes. Because the first-order intensity correlation roots in the single photon's self-interference [9,15],

the present scheme of Fig. 1 satisfies the scope of the delayed-choice experiments as a classical system governed by Poisson statistics as long as coincidence detection is not involved. Due to the same method of polarization projection used in Refs. 7 and 14, the present observations of quantum eraser shed light on quantum mechanics to better understand quantum features such as Bell inequality violation (discussed elsewhere) [14].

Results

Experiments

Figure 1 shows the schematic of the present delayed-choice experiments for quantum eraser in a noninterfering MZI composed of PBSs. Without polarizers (Ps), the scheme is for classical superposition of the distinguishable polarization bases, resulting in no interference fringes. The input photon passing through the 22.5° -rotated quarter-wave plate (QWP) takes only either route inside the MZI randomly via PBS1. In addition, both MZI paths can give random polarization bases of vertical (V) and horizontal (H) components via the $\pm 22.5^\circ$ -rotated half-wave plates (HWPs). Even though the HWP generates ζ or η dependent arbitrary polarization rotation in each MZI path, PBS2 provides only orthogonal polarization bases in the output photons, resulting in no interference fringes on Screens S1 and S2 without Ps. Thus, Fig. 1 satisfies a perfect classical system with distinguishable photons. In coherence optics, this noninterfering phenomenon is known as the Fresnel-Arago law, where orthogonal bases of a physical entity cannot interfere with each other [19]. For the delayed-choice experiments of quantum eraser, the output fields (photons) are independently measured via corresponding polarizers (Ps). The role of Ps is to selectively measure the photon polarization projection onto the polarizer's rotation angle of ξ and θ . This delayed-choice measurement results in interference fringes, where the retrieval of quantum superposition in the noninterfering MZI is proof of the quantum eraser.

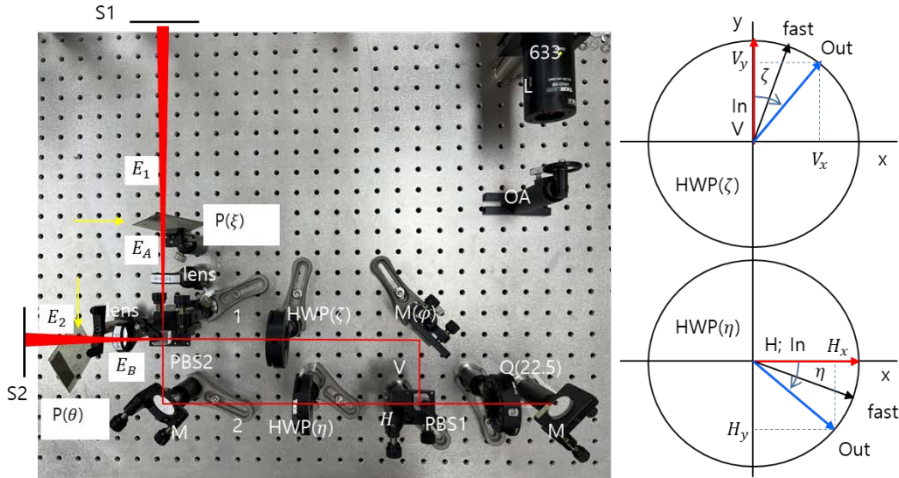


Fig. 1. Schematic of Wheeler's thought experiments of quantum eraser using coherent light. L: laser, OA: optical attenuator, Q: quarter wave plate, M: mirror, PBS: polarizing beam splitter, HWP: half-wave plate, P: polarizer, S: Screen. Inset: HWP controls.

Figure 2 shows experimental demonstrations of the delayed-choice for the quantum eraser in Fig. 1 via polarizers, where the light source is a cw HeNe laser at $\lambda = 632.8$ nm, whose linewidth and polarization is 1 MHz and vertical, respectively. In a typical coherent MZI comprising BSs, the output photons should show interference fringes regardless of the photon characteristics via single photon self-interference [9,15]. This interference fringe is governed by Sorkin's parameters, and the related physics has been intensively studied for Born rule tests [16-18]. As shown in the first column of Fig. 2, the output fields I_A and I_B without Ps show no interference fringes, regardless of HWPs, satisfying the distinguishable photon characteristics by PBS2. Here, $I_B = 0$ without HWPs is because of the role of PBS2, blocking the vertical (horizontal) component of the H- (V-)

polarized photon (not shown): $V_h = H_v = 0$. With proper rotation angles ($\xi; \theta; \zeta; \eta$) of the Ps and HWPs, the a-priori noninterfering MZI turns out to be coherent, resulting in interference fringes in the output ports, as shown in the rest columns of Fig. 2. These are proofs of the delayed-choice for a quantum eraser using cw lights in the present classical model of Fig. 1.

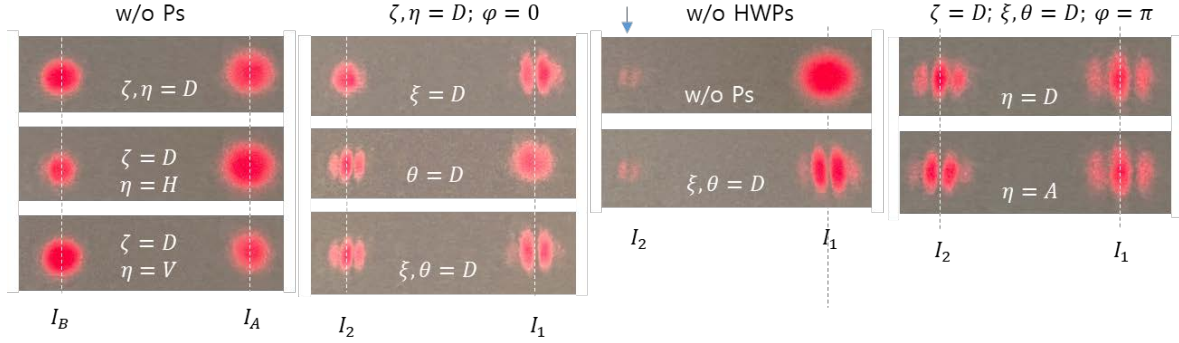


Fig. 2. Experimental demonstrations of delayed-choice for the quantum eraser. I_j is the intensity of E_j . A (D) is for the anti-diagonal (diagonal) in P's rotation from the horizontal axis into a counterclockwise direction.

In Fig. 2, the images are captured from both screens S1 (right) and S2 (left). The first column is for the measured output fields without Ps in Fig. 1. Due to the perfect distinguishable photon characteristics in the non-interfering MZI, there are no interference fringes regardless of HWPs (see the first column). Depending on the rotation angles of HWPs, however, the output intensities change. The second column is with Ps inserted in the output paths of the MZI. The top panel is with only one polarizer in Path A, resulting in an interference fringe in I_1 on Screen S1. The middle panel is for the swapped case with the polarizer in Path B, resulting in an interference fringes in I_2 on Screen S2. The bottom panel is with both polarizers in both paths, resulting in fringes in both I_1 and I_2 . Thus, the role of the polarizer is to retrieve the coherence properties of the MZI, demonstrating the delayed-choice experiments for the quantum eraser. Compared with the first column, nothing changes in the bottom panel except the polarizers inserted in the output ports of MZI. For the captured images, I_1 is intercepted by a mirror and sent to Screen S2. For visualization purposes, a spatial misalignment is intentionally applied for the fringe images.

The third column shows the output field's images without HWPs. The top panel is without polarizers, too, resulting in $I_2 = 0$ due to $V_x = H_y = 0$. Thus, all light travel to output Path A. The dim images of I_2 are caused by imperfect optics, where the unwanted leakage of polarized lights ($\sim 1\%$) results in the dim interference fringes in I_2 . This was also confirmed with φ variation (not shown). As shown, no fringe is observed in I_1 without P. The bottom panel is with P, whose polarization axis is rotated into a diagonal direction, resulting in interference fringes. This is the proof of the delayed-choice for the quantum eraser without HWPs, which is more in line with common understanding.

The last column is with HWPs. The top panel is for 22.5° ($\eta = \zeta = 45^\circ$) rotated HWPs as a reference, resulting in the quantum eraser in both images. The bottom panel is for the anti-diagonal direction of one HWP ($\eta = -45^\circ$) in MZI Path 2, resulting in fringe swap only in I_2 . As shown in *Theory* below, the fringe control is due to $\pm x$ ($\pm y$) components of V (H) via HWP, resulting in the fringe swap only in I_2 , because I_1 has no such components by PBS2 (see Eqs. (1)-(4)). If the ζ choices of HWP is applied between D and A for a fixed η , the fringe swapping is also induced in I_2 (not shown). Therefore, HWPs correlate with output fringes via Ps. The output fringes are also φ -dependent. Depending on $\varphi \in \{0, \pi\}$, both output fringes show swapping (not shown). If the path-length difference of the MZI is beyond the coherence length of the cw laser, no delayed-choice experiments are observed. This means that the concept of the indistinguishability of the particle nature must be satisfied within phase coherence of the wave nature.

Theory

To understand the experimental observations in Fig. 2, the following analytical descriptions are presented for Fig. 1:

$$E_A = \frac{E_0}{\sqrt{2}}(-e^{i\varphi}V_y + H_x), \quad (1)$$

$$E_B = \frac{iE_0}{\sqrt{2}}(H_y + e^{i\varphi}V_x), \quad (2)$$

where V_j and H_j indicate the HWP-resulting random polarization components by HWPs through PBS2. By the rotation angles of HWPs, $V_x = H\cos\zeta\sin\zeta$, $V_y = V\cos^2\zeta$, $H_x = H\cos^2\eta$, and $H_y = H\sin\eta\cos\eta$ result after PBS2. Here, the convention of ζ and η are shown in the Inset of Fig. 1. The term $e^{i\varphi}$ is the path-length difference-caused phase difference between two paths of the original H and V components. Thus, the output intensities are given by $I_A = I_0$ and $I_B = 0$ without HWPs due to $V_h = H_v = 0$. Even with HWPs for Eqs. (1) and (2), no interference fringe results in the output fields due to PBS2, testifying no interaction between orthogonal polarization bases. As a result, the MZI in Fig. 1 satisfies the classical system with distinguishable photon characteristics. If PBS2 is replaced by a BS, the system becomes coherent depending on ζ and η of HWPs, resulting in interference fringes of I_A and I_B .

By inserting Ps in both output ports, polarization projections of the output photons are carried out onto the corresponding polarizers. Thus, the final output fields are modified to:

$$E_1 = \frac{E_0}{\sqrt{2}}(H_x\cos\xi - V_y\sin\xi e^{i\varphi}), \quad (3)$$

$$E_2 = \frac{iE_0}{\sqrt{2}}(-H_y\sin\theta + V_x\cos\theta e^{i\varphi}). \quad (4)$$

Due to P-caused polarization projection onto the common direction for the orthogonal bases in each output field, the initially given noninterfering MZI becomes now coherent, resulting in the following output intensities (see the fringes in Fig. 2):

$$I_1 = \frac{I_0}{2}(\cos^4\eta\cos^2\xi + \cos^4\zeta\sin^2\xi - HV\cos^2\eta\cos^2\zeta\sin 2\xi\cos\varphi) \quad (5),$$

$$I_2 = \frac{I_0}{2}(\sin^2\eta\cos^2\eta\sin^2\theta + \sin^2\zeta\cos^2\zeta\cos^2\theta - HV\sin\eta\cos\eta\sin\zeta\cos\zeta\sin 2\theta\cos\varphi). \quad (6)$$

In Eqs. (5) and (6), the notation with HV is to clarify the origin of coherence excited by Ps for the initially given orthogonal fields.

For $\zeta = \eta = \pm\frac{\pi}{4}$ of HWPs, resulting in the same diagonal (anti-diagonal) polarizations, the output fields of Eqs. (5) and (6) become:

$$I_1 = \frac{I_0}{8}(1 - \sin 2\xi\cos\varphi). \quad (7)$$

$$I_2 = \frac{I_0}{8}(1 + \sin 2\theta\cos\varphi). \quad (8)$$

Thus, both output fields of Eqs. (7) and (8) result in interference fringes as a function of the rotation angle ($\xi; \theta$) of Ps and the MZI path-length difference-caused phase φ (see the last column of Fig. 2).

For $\xi = \theta = \frac{\pi}{4}$ of Ps, resulting in a diagonal polarizations, Eqs. (5) and (6) become:

$$I_1 = \frac{I_0}{2}\left[\frac{1}{2}(\cos^4\eta + \cos^4\zeta) - HV\cos^2\eta\cos^2\zeta\cos\varphi\right], \quad (9)$$

$$I_2 = \frac{I_0}{2}\left[\frac{1}{2}(\sin^2\eta\cos^2\eta + \sin^2\zeta\cos^2\zeta) - HV\sin\eta\cos\eta\sin\zeta\cos\zeta\cos\varphi\right]. \quad (10)$$

Equations (9) and (10) show the function of HWPs and MZI phase φ . For a fixed φ , the orthogonal bases of diagonal ($D, \frac{\pi}{4}$) and anti-diagonal ($A, -\frac{\pi}{4}$) polarizations of HWPs result in the fringe swapping between them only in Eq. (10), as demonstrated in the last column of Fig. 2. I_1 is independent of the D and A of HWPs due to the square and quadruple terms of the sine and cosine functions in Eq. (9). This is actually due to $V_x = H_y = 0$ in Path A for I_1 by PBS2. In summary, the MZI phase φ induces fringe swapping between I_1 and I_2 . However, the swapping with HWP controls applies to only I_2 . For a fixed set of HWPs, the P's basis choice always swaps the fringes in both output fields. The fringe swapping between I_1 and I_2 happens only for opposite basis selections. The above analyses of fringe controls of output fields with HWP, P, and φ have

already been experimentally demonstrated in Ref. 7 using entangled photon pairs. Thus, the equivalence between not only classical and quantum particles but also single photons and cw light is well explained using coherence optics.

Discussion

Indistinguishability and quantum superposition

If PBS2 is replaced by BS in Fig. 1, the HWP itself changes the distinguishable photons into indistinguishable photons, resulting in interference fringes in the output fields of I_A and I_B even without polarizers. This is the general concept of the delayed-choice experiments for quantum eraser. However, PBS2 in Fig. 1 locks the interferometric system in a classical model of distinguishable photons as experimentally demonstrated in Fig. 2 (see the first column). The concept of distinguishability (indistinguishability) corresponds to the incoherence (coherence) nature of the particle (wave) in quantum mechanics. As demonstrated in ‘self-interference’ with a single photon [9], cw-light interference is also rooted in the same physics. Due to the limited Sorkin’s parameter with one input and two output MZI of Fig. 1 [20], the output fringe cannot be distinguished where the input light is a single photon or a cw light. This is why the same delayed-choice experiments have been observed with thermal, coherent, and quantum particles for the first-order intensity correlation. To satisfy delayed-choice experiments, the path-length difference of the MZI must be shorter than the laser linewidth. In other words, coherence of the interferometric system is the bedrock of quantum features in the delayed-choice experiments for coherence retrieval by polarization projections.

Quantum eraser in the PBS-PBS MZI

The role of polarizers applied to the output fields in Fig. 1 is to retrospectively controls the pre-determined non-interfering MZI into coherence by measurement choices of the polarization bases. The observations of the delayed choice in Fig. 2 contradict the cause-effect relation of classical physics. First, the orthogonal polarization-based MZI system strictly prohibits self-interference of a single photon. Second, the retrospective action by the polarizer cannot affect the photon characteristics already passed throughout the MZI. Thus, the observed fringes must violate the causality because the measured photons do not stay inside the MZI anymore. Even though the space-like separation scheme is not involved in Fig. 2, the observed quantum feature cannot be explained by any classical means.

Function of the polarizer

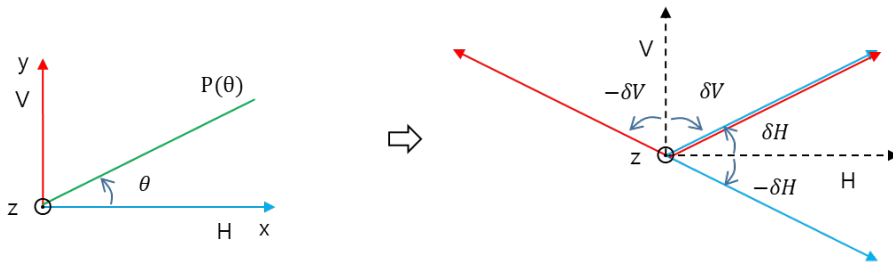


Fig. 3. Measurement choices of polarization bases.

Regarding the role of polarizers with rotation angles ξ and θ in Fig. 1, the resulting interference fringes can be interpreted as polarization projection of orthogonally polarized photons onto the rotated polarizers, resulting in the same polarization direction. To understand this interpretation, each orthogonal polarization basis can be decomposed into an arbitrary superposition state of any set of symmetric polarization components to produce the same polarization basis. In Fig. 3, the θ polarization rotation of the polarizer P rotates measurements through $\pm\delta H$ ($\frac{\pi}{2} \mp \delta V$) from the original H (V), where $\pm\delta H$ ($\pm\delta V$) corresponds to $\pm\theta$ ($\frac{\pi}{2} \mp \theta$). Thus, for

$+\theta$, the opposite components $H - \delta H$ and $V - \delta V$ are perfectly cancelled out, resulting in the constructive interference of $H + \delta H$ and $V + \delta V$. As a result, the role of P is to choose any particular pair of symmetrically superposed polarization components determined by P's rotation angle. Thus, the retrospective measurements by Ps represent selective measurements of the virtually superposed symmetric components of both polarization bases. Regardless of the mean photon number of the cw light, this interpretation applies to each single photon, resulting in self-interference through a noninterfering MZI via polarization projection. Thus, the role of P is a selective measurement of the polarization components.

Conclusion

A classical version of the delayed-choice experiments was experimentally demonstrated for a quantum eraser using cw laser in a noninterfering MZI. The quantum eraser was tested for the output fields of the MZI via polarizer's rotation. For this, HWPs are used for random polarization basis generation in each MZI path. Thus, the observed interference fringes are the evidence of the quantum eraser, violating the cause-effect relation, where the retrospective action of the Ps cannot be understood in classical physics. The violation of the cause-effect relation was in regard to the preset orthogonally polarized MZI composed of a pair of PBSs, where the photons left the MZI before measurements. Analytical solutions were also obtained in a pure coherence approach, where the analyses with polarizers, HWPs, and MZI path length were equivalent to those in Ref. 11 based on entangled photons. Thus, the demonstration of quantum eraser in the present cw scheme is important to understand the mysterious quantum feature belongs to the fundamental concept of indistinguishable single photon in an MZI via single photon self-interference. To interpret the quantum eraser observed, the concept of superposition of symmetrically detuned polarization pairs with respect to the polarizer was applied to the same polarization bases of a photon, resulting in constructive (destructive) interference along (perpendicular to) the polarizer. Thus, the observed quantum eraser could be understood as measurement choices of polarization components via quantum superposition. To satisfy with the quantum features, the path-length difference of MZI had to be shorter than the coherence length of the laser.

Acknowledgment

This work was supported by the ICT R&D program of MSIT/IITP (2021-0-01810), development of elemental technologies for ultrasecure quantum internet and the GIST Research Project in 2022.

Reference

1. P. A. M. Dirac, The principles of Quantum mechanics. 4th ed. (Oxford university press, London, 1958), Ch. 1, p. 9
2. R. P. Feynman, R. Leighton, and M. Sands, The Feynman Lectures on Physics, Vol. III (Addison Wesley, Reading, MA, 1965).
3. J. A. Wheeler, in *Mathematical Foundations of Quantum Theory*, Marlow, A. R. Ed. (Academic Press, 1978), pp. 9-48.
4. M. O. Scully and K. Drühl, Quantum eraser: A proposed photon correlation experiment concerning observation and "delayed choice" in quantum mechanics. *Phys. Rev. A* **25**, 2208-2213 (1982).
5. M. O. Scully, B.-G. Englert, and H. Walther, Quantum optical tests of complementarity. *Nature* **351**, 111-116 (1991).
6. Z. Y. Ou, L. J. Wang, X. Y. Zou, and L. Mandel, Evidence for phase memory in two-photon down conversion through entanglement with the vacuum. *Phys. Rev. A* **41**, 566-568 (1990).
7. T. J. Herzog, P. G. Kwiat, H. Weinfurter, and A. Zeilinger. Complementarity and the quantum eraser. *Phys. Rev. Lett.* **75**, 3034-3037 (1995).
8. Y.-H. Kim, R. Yu, S. P. Kulik, and Y. Shih, Delayed "choice" quantum eraser. *Phys. Rev. Lett.* **84**, 1-5 (2000).

9. P. Grangier, G. Roger, and A. Aspect, Experimental evidence for a photon anticorrelation effect on a beam splitter: A new light on single-photon interferences. *Europhys. Lett.* **1**, 173-179 (1986).
10. T. Peng, H. Chen, Y. Shih, and M. O. Scully, Delayed-choice quantum eraser with thermal light. *Phys. Rev. Lett.* **112**, 180401 (2014)
11. V. Jacques, E. Wu, F. Grosshans, F. Treussart, P. Grangier, A. Aspect, and J.-F. Roch, Experimental realization of Wheeler's delayed-choice gedanken experiments. *Science* **315**, 966-968 (2007).
12. S. Yu, Y.-N. Sun, W. Liu, Z.-D. Liu, Z.-J. Ke, Y.-T. Wang, J.-S. Tang, C.-F. Li, and G.-C. Guo, Realization of a causal-modeled delayed-choice experiment using single photons, *Phys. Rev. A* **100**, 012115 (2019).
13. X. S. Ma, S. Zotter, J. Kofler, R. Ursin, T. Jennewein, C. Brukner, and A. Zeilinger, *Nature Phys.* **8**, 479-484 (2012).
14. T. Kim, M. Fiorentino, and F. N. C. Wong, Phase-stable source of polarization-entangled photons using a polarization Sagnac interferometer. *Phys. Rev. A* **73**, 012316 (2006).
15. W. Ruckner and J. Peidle, Young's double-slit experiment with single photons and quantum eraser. *Am. J. Phys.* **81**, 951-958 (2013).
16. Sinha, U., Couteau, C., Jennewein, T., Lafamme, R. and Weihs, G. Ruling out multi-order interference in quantum mechanics. *Science* **329**, 418-420 (2010).
17. Bo-Sture K. Skagerstam, "On the three-slit experiment and quantum mechanics," *J. Phys. Commun.* **2**, 125014 (2018).
18. Pleinert, M.-O., Rueda, A., Lutz, E. & von Zanthier, J. Testing higher order quantum interference with many-particle states. *Phys. Rev. Lett.* **126**, 190401 (2020).
19. M. Henry, Fresnel-Arago laws for interference in polarized light: A demonstration experiment. *Am. J. Phys.* **49**, 690-691 (1981).
20. R. D. Sorkin, Quantum mechanics as quantum measure theory. *Mod. Phys. Lett.* **9**, 3119-3127 (1994).